

Supplemental Material

Supplemental Figure 1. Assessment of cell purity and fibroblast response to cardiac remodeling in males and females. (A) Heart Weight/Body Weight (HW/BW) ratio of male and female C57BL/6 animals demonstrate increased cardiac hypertrophy after 10 days of swim-training in males and 28 days in females. (B) Picrosirius Red staining of collagen I and III fibers from sections of hearts subjected to indicated conditions (scale bar=100 μ m) (C) Masson's trichrome staining of sections from adult C57BL/6 mice shows no increase in fibrosis after 28 days of swim-training. (D) qRT-PCR to detect *Col1a1* in CFs from C57BL/6 males and females subjected to indicated duration of swim-training or TAC surgery. (E) Echocardiography of male mice demonstrating decreased cardiac function (percent change from baseline) at 10-day TAC compared to sham surgeries. (F) *Myh7/6* and *Cebp β* in CMs from C57BL/6 males subjected to indicated duration of swim-training or TAC surgery. (G) FACs analysis of adherent cells from sedentary C57BL/6 male mice, isolated by differential plating, average percentage from n=3, p<0.0001. (H) FACs analysis of total non-myocyte cell populations in sedentary, swim-trained, and TAC-operated animals, n=3. (I) qRT-PCR to detect *Fsp1* and *Tnnt2*. Relative expression of (J) *Myh6* (cardiomyocyte), (K) *Myh11* (smooth muscle cell), *Cdh5*, and *Pecam1* (endothelial cell) by RNA-sequencing. (L) Relative expression of *Ptprc* (leukocyte) *Il1 β* , *Tnf*, and *Nos2* (inflammatory) by RNA-sequencing. Statistics were performed using 1-way ANOVA and Tukey's post-hoc test. Data represents the mean +/- S.D. *P<0.05; **P<0.01; ***P<0.001; ****P<0.0001.

Supplemental Figure 2. Statistically significant pairwise comparisons and FPKM plots of individual genes from IPA canonical pathways. (A) For a pairwise comparison, significant genes were retained if at least one FPKM value in a comparison per gene was greater than 1 and q-value < 0.05. Furthermore, in pairwise comparisons involving the control, retained genes were unique to the stimulus (swim or TAC) and differentially expressed at either the early (3-4 days) or later (10 day) time points. Numbers in parentheses for control vs. 10-day TAC and control vs 10-day swim indicate total number of genes (2454 total (1591 upregulated and 863 downregulated) in swim vs. control, and 4051 total (2569 upregulated and 1482 downregulated) in TAC vs. control including those that appear in both lists and change in the same direction. By removing genes that appeared in both lists, the gene lists were reduced to 379 (223 upregulated and 156 downregulated) and 1976 (1206 upregulated and 770 downregulated) for swim vs. control and TAC vs. control, respectively. Black half-circles indicate numerator in a pairwise comparison. Log₁₀ (FPKM) values for individual genes in (B) NRF2-mediated oxidative stress response, (C) Hepatic Fibrosis/Hepatic Stellate Cell Activation, (D) RhoA signaling, and (E) ILK signaling. Colored dots indicate presence of gene in "molecules" field of IPA output for 10-day swim vs. pooled control (dark blue), 10-day TAC vs. pooled control (pink), and 10-day swim vs. 10-day TAC (cyan) lists. Widest point of directional arrowhead indicates FPKM of gene in pooled control, and tip of arrowhead indicates FPKM of gene in 10-day swim CFs (dark blue) or 10-day TAC CFs (pink).

Supplemental Figure 3. Physiological and pathological remodeling differentially regulate transcriptional activity in CFs. Identification of enriched transcription factor binding sites in the proximity of genes that are enriched in CFs between 10-day TAC vs. sham controls or 10-day swim vs. sedentary controls by Motif analysis using HOMER 2.0.

Supplemental Figure 4. Evaluation of TGF- β 1, IGF-1 and ROS signaling in cardiac fibroblasts in vitro and in vivo. (a) Representative Western blot and (b) quantification of total cell lysate (TCL) demonstrates phosphorylation of S473-AKT and SMAD/3 in response to ROS, IGF-1/ROS, or TGF- β 1/ROS treatment of neonatal mouse CFs. (c) Representative Western blot and (d) quantification of NRF2 immunoprecipitation demonstrates decreased ubiquitination of NRF2 after ROS or IGF-1/ROS treatment compared to control or TGF- β 1/ROS treated neonatal mouse CFs. (e) Western blot of phosphorylated p38 in CFs pooled from three animals per condition (sedentary, 10-day swim, or 10-day TAC). Statistics were performed using 1-way ANOVA and Tukey's post-hoc test. Data represents the mean \pm S.D. * P <0.05; ** P <0.01; *** P <0.001; **** P <0.0001.

Supplemental Figure 5. Metallothionein 1 and 2 deletion in mice leads to exercise-induced cardiac fibrosis. (A) Heart Weight/Tibia Length (HW/TL) ratio of MTKO and WT animals at 28-day swim shows no significant difference in males or females due to loss of MT1/2. qRT-PCR of whole ventricle tissue to detect (B-E) *Cebpb*, *Myh7/6*, *Nppa*, and *Nppb* indicate that the swim-training regimen is not a pathological stimulus. (F) Cardiomyocyte cross-sectional area of sedentary and 28 day swim WT and MTKO males. Echocardiography measurements of (G) left ventricular mass in MTKO males, and (H) ejection fraction and (I) fractional shortening in females after swim. (J-L) Quantification of Picosirius Red staining from similar regions in the left ventricular free wall in the absence of physiological stress from MTKO (n=2) and WT (n=2) sedentary male hearts suggests no baseline fibrosis in (J) interstitial, (K) epicardial, and (L) perivascular regions. (M) Quantification of PDGFR α + cells in sedentary and 28 day swim-trained 129 and MTKO animals. (N) HW/TL of 129 and MTKO animals after 28 days of treadmill running. (O) Echocardiography of treadmill-exercised WT and MTKO show no change in ejection fraction over 28 days. (P) Treadmill fatigue test after 19 days of exercise demonstrate that MTKO animals fatigue earlier than WT animals. Statistics in (A-F,M-N) were performed using 1-way ANOVA and Tukey's post-hoc test. Statistics in (G-L,O) were performed using 2-way ANOVA and Tukey's post-hoc test. Statistics in (J-L,P) were performed using student's t-test. Data represents the mean \pm S.D. * P <0.05; ** P <0.01; *** P <0.001.

Supplemental Figure 6. Model summarizing the cardioprotective effects of CF secreted MTs that is maintained in healthy hearts and lost in disease.

Supplemental Table 1. List of genes found in heat map by cluster number.

Supplemental Table 2. Primers used for qRT-PCR.

Supplemental Table 3. Patient data for human heart samples. DCM – dilated cardiomyopathy, ISCH – ischemic heart failure. HF – heart failure. HF – heart failure.

Supplemental Materials and Methods

Animals

All animal experiments were approved by the University Committee on Animal Resources at the University of Rochester. Homozygous MTKO animals on a 129SvJ background were described previously and obtained from Jackson Laboratories (#002211) (1). 129SvJ and C57BL/6 animals were also obtained from Jackson Laboratories. MTKO and 129SvJ animals were maintained as separate strains and backcrossed for at least 4 generations before use.

Human Samples

Human heart tissue was obtained from the Kaufman Center for Heart Failure Tissue Bank at Cleveland Clinic, with Institutional Review Board (IRB) approval and patient consent (Cleveland Clinic IRB approval number: 2378). Failing human heart tissue was obtained from left ventricular assist device implantation cores and cardiac transplant recipients, and non-failing tissue was obtained from unmatched organ donors. A total of 35 patient samples were used in this study, with 17 control patients that died for reasons unrelated to cardiac disease, and 18 patients that met the clinical requirements for either LVAD implantation or heart transplant. Of these 35 patients, 13 were female and 22 were male, ranging in age from 30-67 years of age. All tissue was procured in the operating room after cardioplegic arrest of the heart and was transported quickly to the laboratory, where it was frozen in liquid nitrogen.

TAC, MI, and Swim Models

After administering anesthesia, transverse aortic constriction (TAC) is performed via a left thoracotomy by placing a (6-0 silk) ligature securely around the trans-aorta and a 27-gauge needle, causing complete occlusion of the aorta. The needle is removed, restoring a lumen with severe stenosis. TAC sham surgeries were performed by passing the suture around the aorta without ligating. Myocardial infarction (MI) was performed by intramural ligation of the left anterior descending coronary artery 2 mm from its origin with a 9-0 proline suture. The swim model was performed as previously described with slight modifications, where animals were conditioned to exercise by increasing the time spent swimming each day (2). Day 1 corresponded to 2 x 10 min swim sessions and increased 10 minutes twice a day until animals were swimming 2 x 90 min per day.

Primary Cell Isolation

Adult mouse ventricular cardiomyocytes and fibroblasts were isolated using a Langendorff apparatus to obtain a single cell suspension as described previously (Casey et al., 2010) with minor modifications. Briefly, the heart was removed from the animal, and the aorta cannulated and secured on a blunted 21G needle. The heart was perfused with perfusion buffer and digested with 1mg/mL collagenase II (305U/μg, Worthington Biochemicals) at 37°C. The ventricular tissue was then removed from the

cannula, shredded using forceps, and passed through a 100 μ m filter. Cardiomyocytes were separated by gravity sedimentation for 15 minutes at 37°C and the remaining supernatant was centrifuged at 1000rpm for 5 minutes at 4°C to pellet the non-myocyte population. Cardiac fibroblasts were isolated by plating the resuspended pellet for 2 hours at 37°C in DMEM/10% FBS and washing the attached cells (fibroblasts) three times with 1xPBS before RNA isolation.

Neonatal mouse ventricular fibroblasts and cardiomyocytes were isolated from P0 neonates. The ventricles were minced in DMEM and digested in 4 changes of 0.8mg/mL collagenase II (305U/ μ g, Worthington Biochemicals) at 37°C in a small glass vial with a mini stir bar. Cells from each change were pooled and collected on ice, filtered through a 70 μ m filter, and pelleted. Neonatal ventricular fibroblasts isolated by differential plating and neonatal CMs were removed from the adherent fibroblasts plated on gelatin coated tissue culture plastic.

Human cardiac fibroblasts were isolated from human heart tissue that would have otherwise been discarded during left ventricle assist device implantation at the University of Rochester Medical Center, with Institutional Review Board (IRB) approval and patient consent (University of Rochester IRB approval number: 52958). Briefly, 1g pieces from fresh cores were minced and digested using the Miltenyi system in 10mL (mouse neonatal heart dissociation kit and gentleMACS Octo Dissociator with heaters, program 37C_mr_NHDK_1) according to manufacturer's directions. Viable human cardiac fibroblasts were isolated by differential plating for 2 hours at 37°C in full culture medium (DMEM/10%FBS/1mM sodium pyruvate), and passaged an average of 3-5 times before use but always used before passage 7.

RNA Isolation

RNA was isolated from CFs and CMs by Trizol/chloroform isolation. Genomic DNA was removed by treating the RNA with Turbo DNase (Ambion). cDNA was generated from 500-1000ng RNA using iScript Reverse Transcriptase kit (BioRad) as per manufacturer's recommendations.

qRT-PCR

Reactions were performed with BioRad SYBR-Green master mix on a BioRad CFX Connect per manufacturer's recommendations. Primers used for qRT-PCR are listed in Supplementary Table 2.

Stranded mRNA-seq

Total RNA was isolated using the RNeasy Plus Kit and genomic DNA removed using gDNA columns (Qiagen, Valencia, CA) per manufacturer's recommendations. RNA concentration and quality was assessed with the Agilent Bioanalyzer (Agilent, Santa Clara, CA) and only samples with RIN>8.5 were used for sequencing. Illumina compatible library construction was performed using the TruSeq Stranded mRNA Sample Preparation Kit (Illumina, San Diego, CA) per manufacturer's recommendation and sequenced using an Illumina HiSeq2500.

NGS Data Processing and Alignment

Raw reads generated from the Illumina HiSeq2500 sequencer were demultiplexed using `configurebcl2fastq.pl` version 1.8.4. Low complexity reads and vector contamination were removed using sequence cleaner (`seqclean`) and the NCBI univec database, respectively. The FASTX toolkit (`fastq_quality_trimmer`) was applied to remove bases with quality scores below Q=13 from the end of each read. Processed/cleaned reads were then mapped to the mouse mm10 genome build with SHRiMP version 2.2.3 with the following parameters: "--qv-offset 33 --all-contigs". Differential expression analysis is performed using Cufflinks version 2.0.2; specifically, `cuffdiff2` and usage of the general transfer format (GTF) annotation file for the given reference genome with the following parameters: "--FDR 0.05 -u -b GENOME". Analysis and visualization (including clustering) of derived NGS data was performed with Matlab (The Mathworks, Natick MA) and PRISM (GraphPad, San Diego CA). The RNA-Seq data from this publication have been submitted to the Gene Expression Omnibus (GEO) database (GEO GSE89885).

Antibodies

Primary antibodies for immunofluorescence were as follows: mouse anti-FLAG M2 (Sigma, 1:500), mouse IgG (Jackson ImmunoResearch 1mg/ml, 1:500). Secondary antibodies used for immunofluorescence were Alexa 488-conjugated goat anti-mouse (Invitrogen 1:200), Alexa 594-conjugated goat anti-phalloidin (Invitrogen 1:200), and DAPI (Invitrogen 1mg/ml, 1:1000). Primary antibodies used for western blotting were as follows: NRF2 (Abcam ab31163, 1:1000), ubiquitin (Cell Signaling 3936, 1:2000), phospho-p38 (Cell Signaling 9211, 1:500), total p38 (Cell Signaling 9212, 1:1000), phospho-AKT (Cell Signaling 9271, 1:1000), AKT (Cell Signaling 9272, 1:2000), phospho-SMAD3 (Cell Signaling 3101, 1:1000), SMAD3 (Cell Signaling 3103, 1:2000), GAPDH (Millipore MAB374 1:50,000), lamin A/C (Cell Signaling 4777, 1:2500), β III-tubulin (Abcam ab52901, 1:20,000).

MT peptide rescue

Neonatal mouse CMs were isolated and plated at 50,000 cells/well in gelatin coated 96-well black sided tissue culture plates. The following day, unattached CMs were washed off and the surviving CMs pre-treated overnight with designated concentrations of full-length rabbit MT2A (Enzo). Two days post-isolation, the CMs were treated with 0, 125 or 250 μ M H₂O₂ (Sigma) with or without full-length rabbit MT2A for 1 hour at 37°C. Myocytes were then briefly washed once and cultured in normal neonatal CM media for 24 hours without H₂O₂ or MT2A at 37°C before measuring cell viability using CyQuant assay (Invitrogen) on a BMG FluoSTAR OPTIMA plate reader per manufacturer's instructions.

Cell Culture

NIH-3T3 cells were transfected 18 hours post-plating with 15 μ g of plasmid DNA (N-FLAG-MT, N-FLAG, or N-FLAG-MKL1) using Mirus X2 Transfection Reagent as per manufacturer's protocol. For conditioned media experiments, NIH-3T3s were cultured in 10mL serum-free neonatal mouse CM media with 10 μ M MG-132 for 24 hours to accumulate secreted proteins in the media. Conditioned media was then collected and concentrated to 350 μ L in Ambion concentrators with a 3kDa cutoff. Neonatal mouse

CMs were isolated and plated in laminin-coated MAT-TEK glass bottom petri dishes at a density of 200,000 per dish. The following day, unattached CMs were washed off and the surviving CMs cultured in culture media (DMEM/10%FBS/1%L-glutamine/1%pen-strep) for 24-48 hours. N-FLAG-MT in CMs was detected by culturing CMs with concentrated conditioned media from transfected 3T3s for 4 hours at 37°C. For MF activation experiments, NIH-3T3s were treated with 10ng/mL TGF-β1 24 hours after transfection with FLAG-Mt1 and RNA collected 24 hours after treatment.

Immunofluorescence

CMs were then washed three times with 1xPBS and fixed with 4% PFA/1xPBS for 10 min at room temperature. Cells were then permeabilized with 0.5% saponin/1xPBS for 5 min and washed three times with 1xPBS. Cells were blocked in 3% BSA/1xPBS, then primary antibody diluted in blocking buffer. After washing three times with 0.05% saponin/1xPBS, CMs were incubated with secondary antibody, washed again three times with 0.05% saponin/1xPBS, treated with DAPI, and visualized by confocal microscopy using an Olympus Fluoview FV1000.

FITC-conjugated isolectin B4 (Sigma L2879 1:100) and FITC-conjugated sheep anti-von Willebrand Factor (Abcam ab8822 1:50) were combined to stain vasculature of MTKO and WT heart sections.

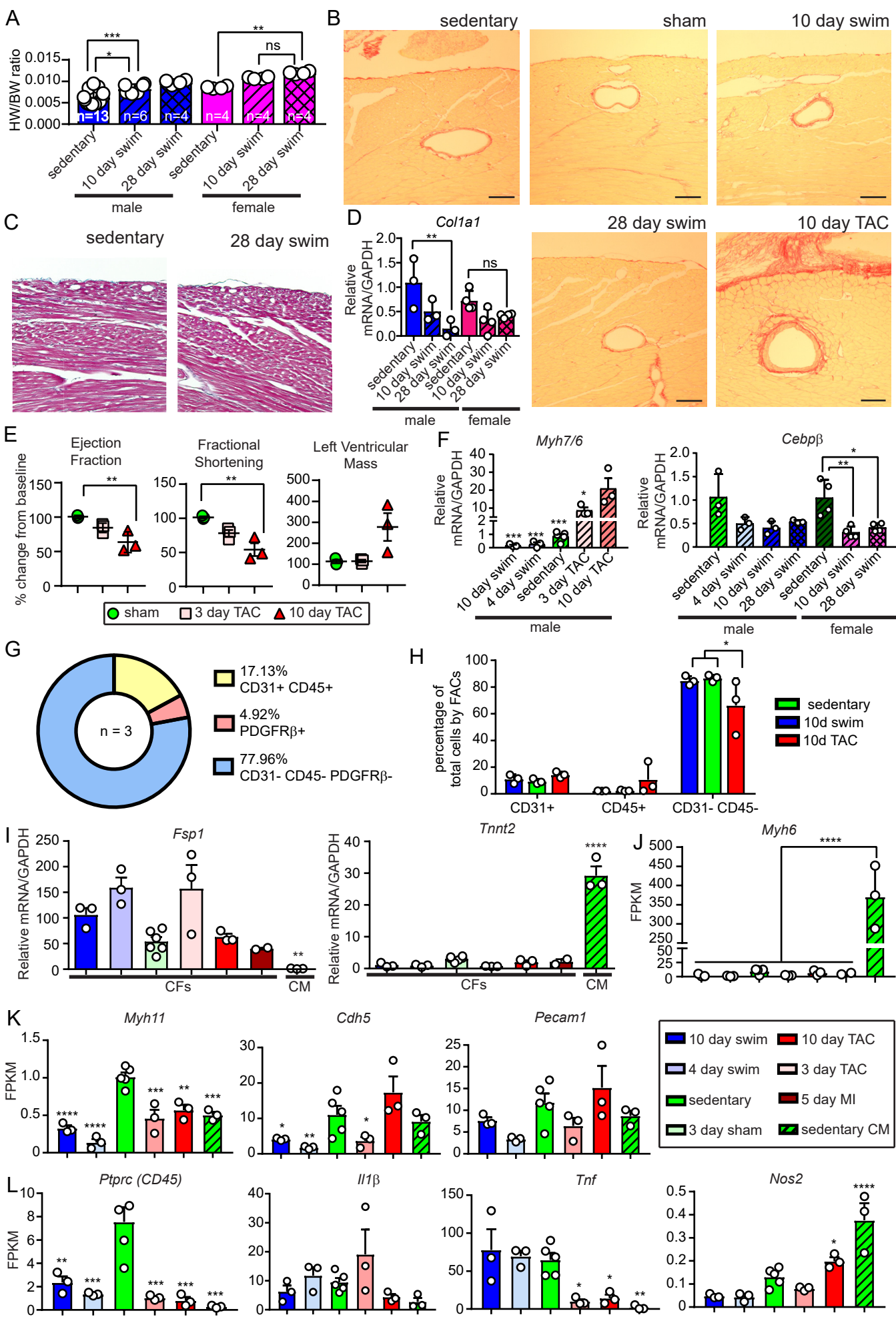
ImageJ quantification of images

Polarized light images of fibrosis of Picrosirius Red stained sections were quantified using ImageJ as described previously (3). Histological sections were blinded and stained, and three independent areas were marked for quantification: vascular wall, epicardial, and interstitial, where the interstitial area was determined by the total area minus the area for the vascular wall and epicardium. Vessel density of MTKO and 129 animals after swim-training was quantified by creating, measuring, and averaging binary masks taken from 5 separate images from the left ventricular free wall.

Supplemental References

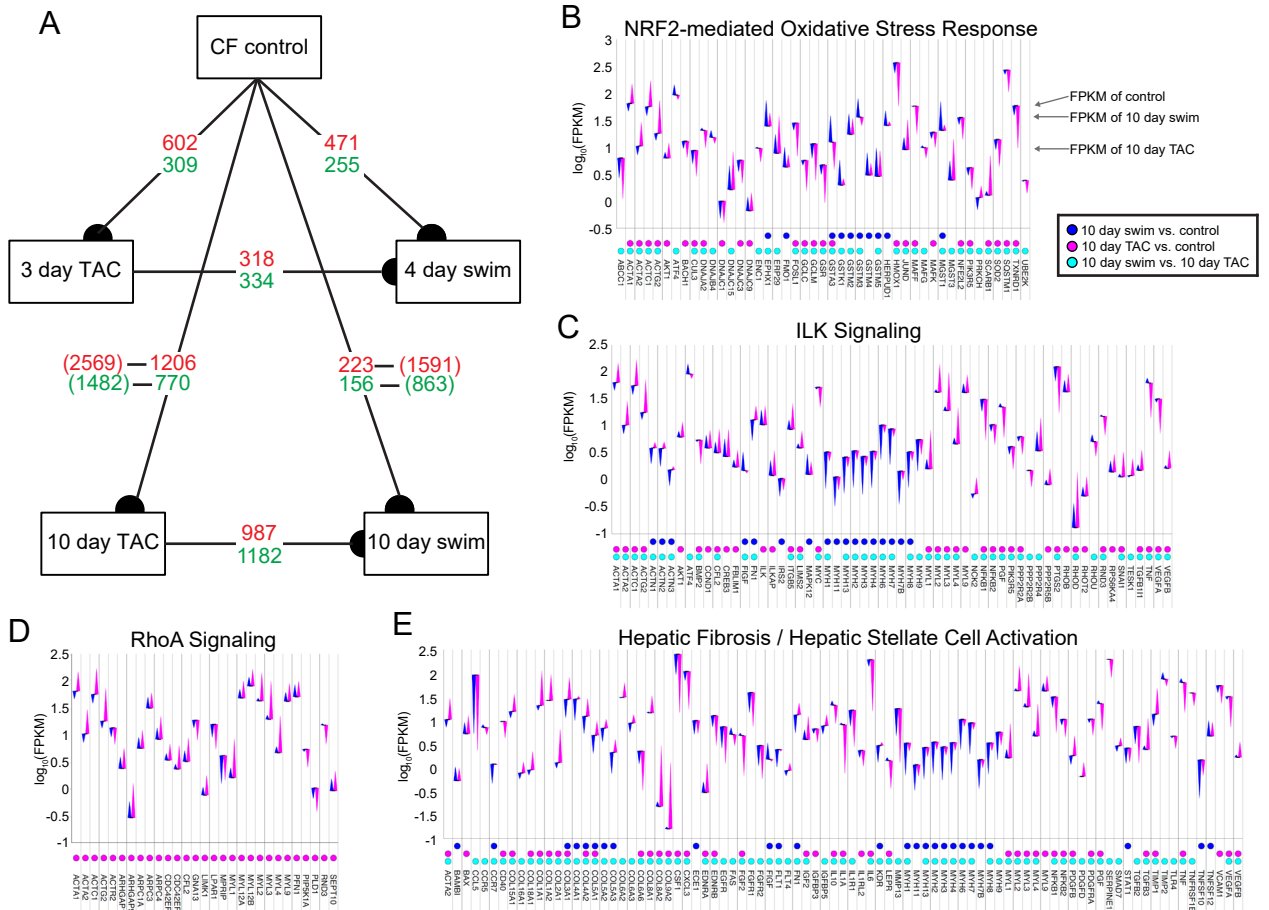
1. Masters BA, Kelly EJ, Quaife CJ, Brinster RL, and Palmiter RD. Targeted disruption of metallothionein I and II genes increases sensitivity to cadmium. *Proc Natl Acad Sci U S A*. 1994;91(2):584-8.
2. Kaplan ML, Cheslow Y, Vikstrom K, Malhotra A, Geenen DL, Nakouzi A, Leinwand LA, and Buttrick PM. Cardiac adaptations to chronic exercise in mice. *The American journal of physiology*. 1994;267(3 Pt 2):H1167-73.
3. Smolock EM, Burke RM, Wang C, Thomas T, Batchu SN, Qiu X, Zettel M, Fujiwara K, Berk BC, and Korshunov VA. Intima modifier locus 2 controls endothelial cell activation and vascular permeability. *Physiol Genomics*. 2014;46(17):624-33.

Supplemental Figure 1



Supplemental Figure 1. Assessment of cell purity and fibroblast response to cardiac remodeling in males and females. (A) Heart Weight/Body Weight (HW/BW) ratio of male and female C57BL/6 animals demonstrate increased cardiac hypertrophy after 10 days of swim-training in males and 28 days in females. (B) Picosirius Red staining of collagen I and III fibers from sections of hearts subjected to indicated conditions (scale bar=100 μ m) (C) Masson's trichrome staining of sections from adult C57BL/6 mice shows no increase in fibrosis after 28 days of swim-training. (D) qRT-PCR to detect *Col1a1* in CFs from C57BL/6 males and females subjected to indicated duration of swim-training or TAC surgery. (E) Echocardiography of male mice demonstrating decreased cardiac function (percent change from baseline) at 10-day TAC compared to sham surgeries. (F) *Myh7/6* and *Cebpb* in CMs from C57BL/6 males subjected to indicated duration of swim-training or TAC surgery. (G) FACS analysis of adherent cells from sedentary C57BL/6 male mice, isolated by differential plating, average percentage from n=3, $p < 0.0001$. (H) FACS analysis of total non-myocyte cell populations in sedentary, swim-trained, and TAC-operated animals, n=3. (I) qRT-PCR to detect *Fsp1* and *Tnt2*. Relative expression of (J) *Myh6* (cardiomyocyte), (K) *Myh11* (smooth muscle cell), *Cdh5*, and *Pecam1* (endothelial cell) by RNA-sequencing. (L) Relative expression of *Ptpcr* (leukocyte), *Il1 β* , *Tnf*, and *Nos2* (inflammatory) by RNA-sequencing. Statistics were performed using 1-way ANOVA and Tukey's post-hoc test. Data represents the mean \pm S.D. * $P < 0.05$; ** $P < 0.01$; *** $P < 0.001$; **** $P < 0.0001$.


Supplemental Figure 2







Supplemental Figure 2. Statistically significant pairwise comparisons and FPKM plots of individual genes from IPA canonical pathways. (A) For a pairwise comparison, significant genes were retained if at least one FPKM value in a comparison per gene was greater than 1 and q -value < 0.05 . Furthermore, in pairwise comparisons involving the control, retained genes were unique to the stimulus (swim or TAC) and differentially expressed at either the early (3-4 days) or later (10 day) time points. Numbers in parentheses for control vs. 10-day TAC and control vs. 10-day swim indicate total number of genes (2454 total (1591 upregulated and 863 downregulated) in swim vs. control, and 4051 total (2569 upregulated and 1482 downregulated) in TAC vs. control including those that appear in both lists and change in the same direction. By removing genes that appeared in both lists, the gene lists were reduced to 379 (223 upregulated and 156 downregulated) and 1976 (1206 upregulated and 770 downregulated) for swim vs. control and TAC vs. control, respectively. Black half-circles indicate numerator in a pairwise comparison. Log₁₀ (FPKM) values for individual genes in (B) NRF2-mediated oxidative stress response, (C) Hepatic Fibrosis/Hepatic Stellate Cell Activation, (D) RhoA signaling, and (E) ILK signaling. Colored dots indicate presence of gene in “molecules” field of IPA output for 10-day swim vs. pooled control (dark blue), 10-day TAC vs. pooled control (pink), and 10-day swim vs. 10-day TAC (cyan) lists. Widest point of directional arrowhead indicates FPKM of gene in pooled control, and tip of arrowhead indicates FPKM of gene in 10-day swim CFs (dark blue) or 10-day TAC CFs (pink).

Supplemental Figure 3

10 day swim CF vs sedentary CF

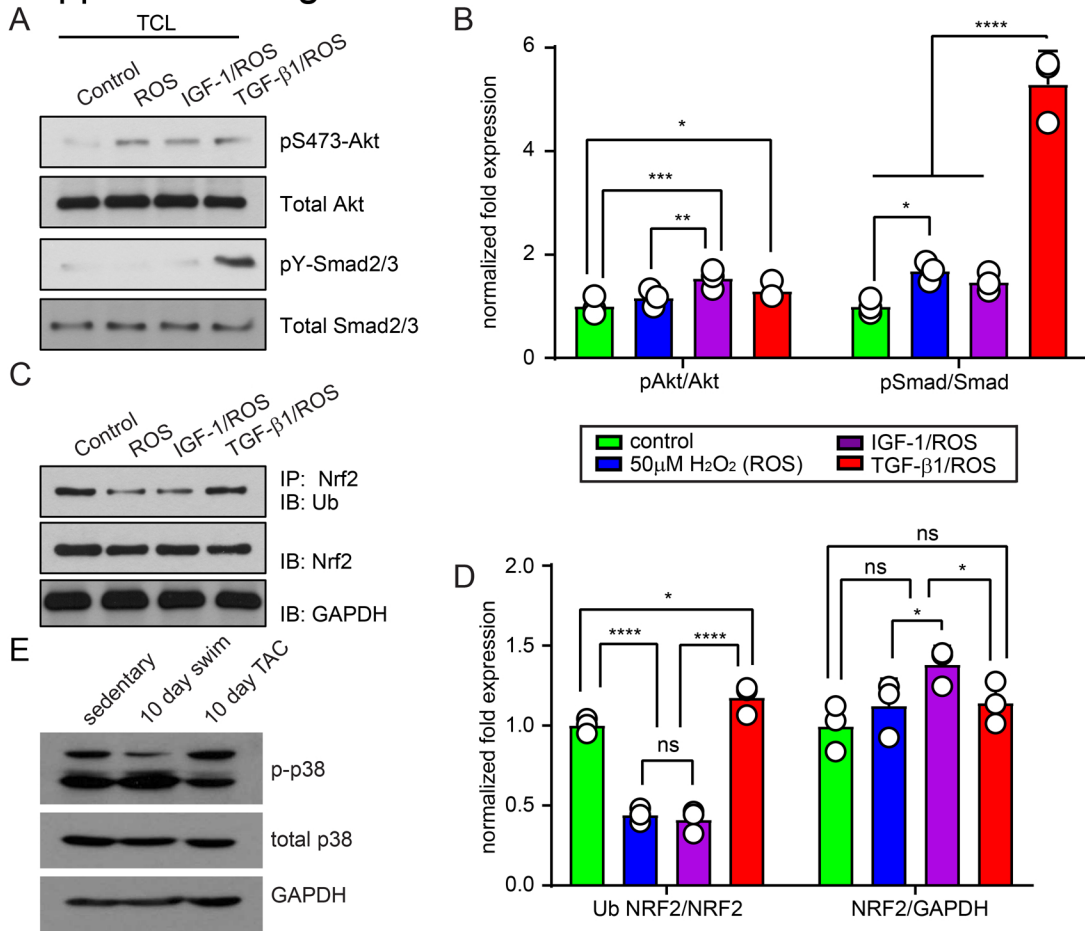
Rank	Motif	Name	p-value	q-value (Benjamini)	% target sequences with motif	% background sequences with motif
1		ZFX(ZF)/mES-Zfx-ChIP-Seq (GSE11431)	1e-3	0.2556	40.19%	36.31%

10 day TAC CF vs 3 day TAC sham CF

Rank	Motif	Name	p-value	q-value (Benjamini)	% target sequences with motif	% background sequences with motif
1		CArG(MADS)/PUER-Srf-ChIP-Seq (Sullivan_et_al)	1e-4	0.0231	13.45%	10.86%
2		ZFX(ZF)/mES-Zfx-ChIP-Seq (GSE11431)	1e-3	0.0367	43.52%	39.88%
3		GFY-Staf (? ,Zf)	1e-2	0.6807	1.37%	0.83%
4		Unknown-ESC-element(?)/mES-Nanog-ChIP-Seq (GSE11724)	1e-2	0.6807	22.10%	20.01%

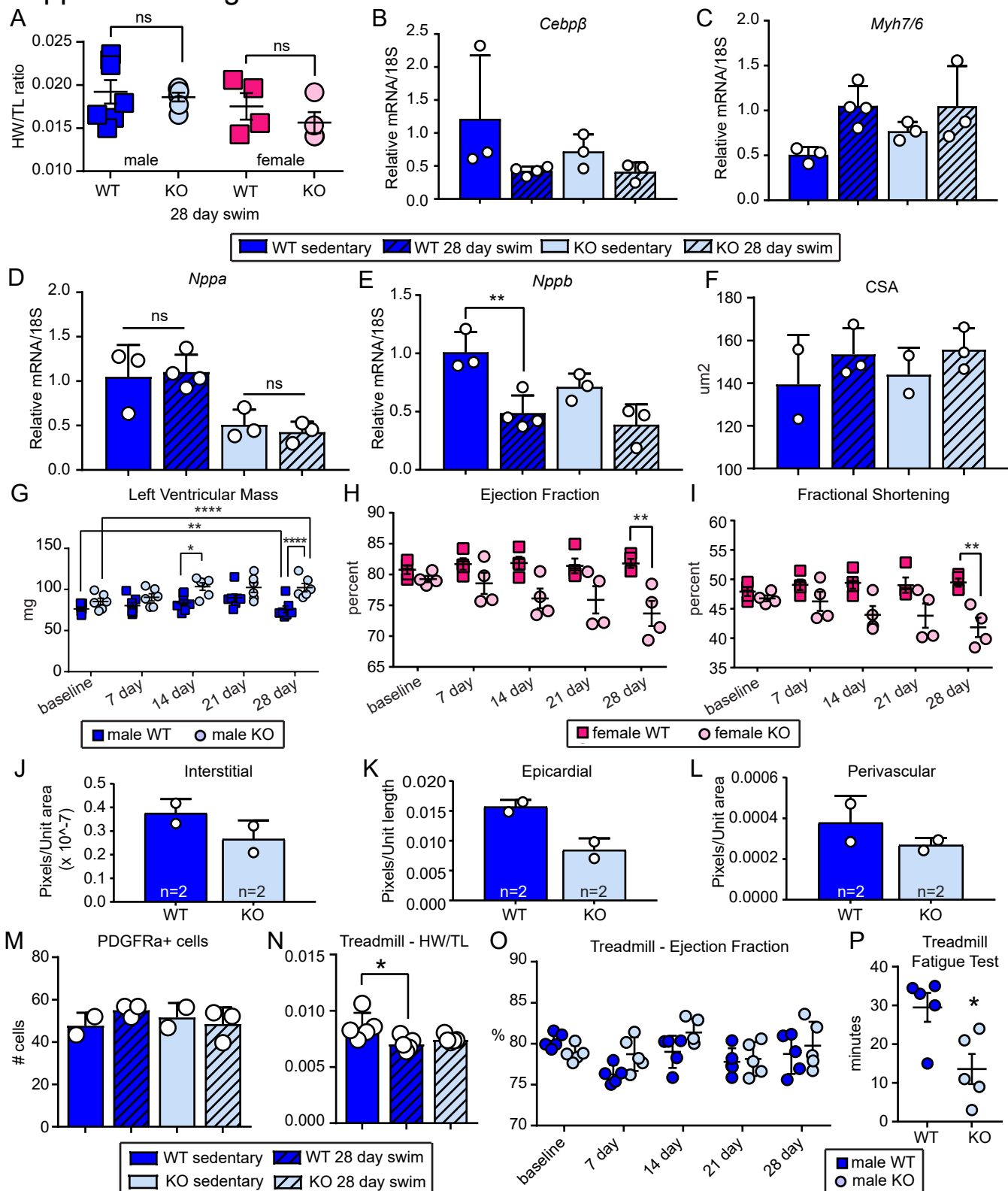
Supplemental Figure 3. Physiological and pathological remodeling differentially regulate transcriptional activity in CFs. Identification of enriched transcription factor binding sites in the proximity of genes that are enriched in CFs between 10-day TAC vs. sham controls or 10-day swim vs. sedentary controls by Motif analysis using HOMER 2.0.

Supplemental Figure 4

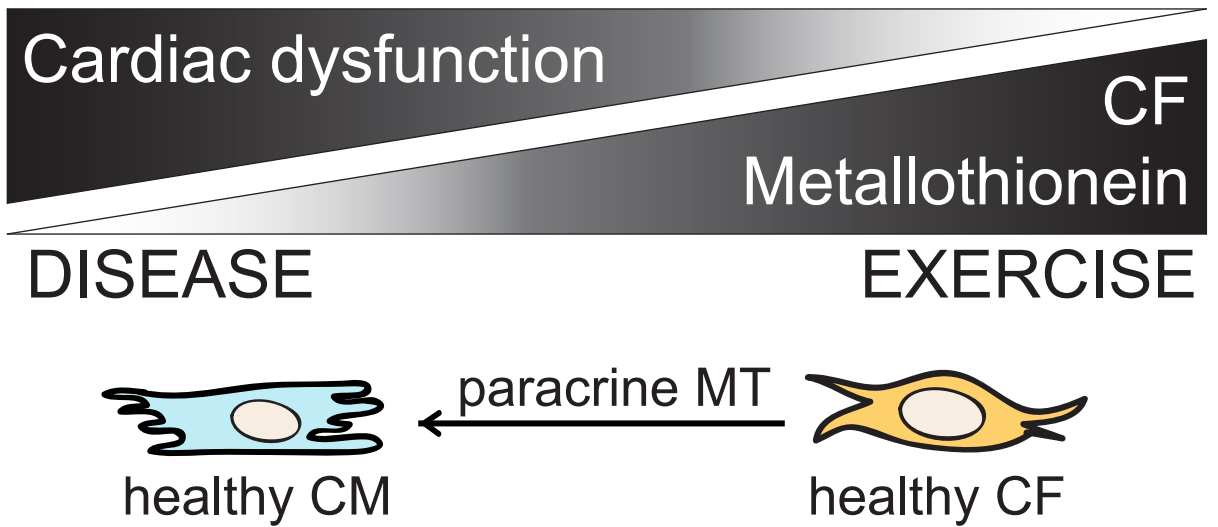


Supplemental Figure 4. Evaluation of TGF- β 1, IGF-1 and ROS signaling in cardiac fibroblasts in vitro and in vivo. (A) Representative Western blot and (B) quantification of total cell lysate (TCL) demonstrates phosphorylation of S473-Akt and Smad2/3 in response to ROS, IGF-1/ROS, or TGF- β 1/ROS treatment of neonatal mouse CFs. (C) Representative Western blot and (D) quantification of NRF2 immunoprecipitation demonstrates decreased ubiquitination of NRF2 after ROS or IGF-1/ROS treatment compared to control or TGF- β 1/ROS treated neonatal mouse CFs. (E) Western blot of phosphorylated p38 in CFs pooled from three animals per condition (sedentary, 10-day swim, or 10-day TAC). Statistics were performed using 1-way ANOVA and Tukey's post-hoc test. Data represents the mean \pm S.D. *P<0.05; **P<0.01; ***P<0.001; ****P<0.0001.

Supplemental Figure 5



Supplemental Figure 5. Metallothionein 1 and 2 deletion in mice leads to exercise-induced cardiac fibrosis. (A) Heart Weight/Tibia Length (HW/TL) ratio of MTKO and WT animals at 28-day swim shows no significant difference in males or females due to loss of MT1/2. qRT-PCR of whole ventricle tissue to detect (B-E) *Cebpb*, *Myh7/6*, *Nppa*, and *Nppb* indicate that the swim-training regimen is not a pathological stimulus. (F) Cardiomyocyte cross-sectional area of sedentary and 28 day swim WT and MTKO males. Echocardiography measurements of (G) left ventricular mass in MTKO males, and (H) ejection fraction and (I) fractional shortening in females after swim. (J-L) Quantification of Picrosirius Red staining from similar regions in the left ventricular free wall in the absence of physiological stress from MTKO (n=2) and WT (n=2) sedentary male hearts suggests no baseline fibrosis in (J) interstitial, (K) epicardial, and (L) perivascular regions. (M) Quantification of PDGFR α cells in sedentary and 28 day swim-trained 129 and MTKO animals. (N) HW/TL of 129 and MTKO animals after 28 days of treadmill running. (O) Echocardiography of treadmill-exercised WT and MTKO show no change in ejection fraction over 28 days. (P) Treadmill fatigue test after 19 days of exercise demonstrate that MTKO animals fatigue earlier than WT animals. Statistics in (A-F,M-N) were performed using 1-way ANOVA and Tukey's post-hoc test. Statistics in (G-L,O) were performed using 2-way ANOVA and Tukey's post-hoc test. Statistics in (J-L,P) were performed using student's t-test. Data represents the mean +/- S.D. *P<0.05; **P<0.01; ***P<0.001.



Supplemental Figure 6. Model summarizing the cardioprotective effects of CF secreted MTs that is maintained in healthy hearts and lost in disease.

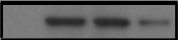
Supplemental Table S2. Primers used for qRT-PCR

primer name	species	sequence (5' - 3')
hCol1a2 qF	human	TGCTGCTCAGTATGATGGAAA
hCol1a2 qR	human	CAGGTCCTTGGAAACCTTGA
hMt2a qF1	human	CTCCAAGTCCCAGCGAACC
hMt2a qR1	human	CAGGAGCAGTTGGGATCCAT
hNppa qF1	human	TGTACAATGCCGTGTCCAAC
hNppa qR1	human	TCTTCATTCCGGCTCACTGAG
hPostn qF	human	TGGAAACCATCGGAGGCAAA
hPostn qR	human	GAATCGCACCGTTTCTCCCT
hsActa2 qF	human	CAGCCAAGCACTGTCAGG
hsActa2 qR	human	CAATGGATGGGAAAACAGC
hTCF21 qF	human	TCCAGCTACATCGCCCACT
hTCF21 qR	human	CATAAAGGGCCACGTCAGGTT
mActa2 qF	mouse	GTT CAG TGG TGC CTC TGT CA
mActa2 qR	mouse	ACT GGG ACG ACA TGG AAA AG
mCEBPb qF	mouse	ACGACTTCTCTCCGACCTCT
mCEBPb qF	mouse	CGAGGCTCACGTAACCGTAGT
mCol1a1 for	mouse	TAG GCC ATT GTG TAT GCA GC
mCol1a1 rev	mouse	ACA TGT TCA GCT TTG TGG ACC
mGAPDH qF	mouse	CGT GCC GCC TGG AGA AAC
mGAPDH qR	mouse	TGG GAG TTG CTG TTG AAG TCG
mGsta2	mouse	BioRad PrimePCR assay
mGsta2	mouse	qMmuCED0041042
mGsta3 qF	mouse	GGCTGAGCAGGGCTGATATT
mGsta3 qR	mouse	ACTCTGTTCTCAGCGCTTT
mGsta4 qF	mouse	TGATTGCCGTGGCTCCATTTA
mGsta4 qR	mouse	CAACGAGAAAAGCCTCTCCGT
mGstm1 qF	mouse	TTTGTCTGCCCACGTTTCT
mGstm1 qR	mouse	CGGACGTTCCAGTATCCCAG
mGstt1 qF	mouse	AGGCTCGTGCTCGTGTAGA
mGstt1 qR	mouse	CAGGGAACATCACCTTATGCC
h/mMt1 qF2	mouse and human	CCCCAACTGCTCCTGCTC
h/mMt1 qR2	mouse and human	CAGCTCTTCTGCAGGAGGT
mMt2 qF	mouse	CCATATCCCTTGAGCCAGAAA
mMt2 qR	mouse	TAGGAGCGTGATGGAGAGAA
mNppa qF	mouse	TTCAAGAACCTGCTAGACCACC
mNppa qR	mouse	ATCTATCGGAGGGGTCCCAG
mPostn qF	mouse	GCAAACCACTTTCACCGACC
mPostn qR	mouse	CGTTGGTCCATGCTCAGAGT
mS100a4_qF	mouse	CTTCTCTCTCTTGGTCTGGTC
mS100a4_qR	mouse	TTTGTGGAAGGTGGACACAA
mTcf21_qF	mouse	CATTCACCCAGTCAACCTGA
mTcf21_qR	mouse	CCACTTCCTCAGGTCATTCTC
mTnT_qF	mouse	TCGACCACCTGAATGAAGACC
mTnT_qR	mouse	TTCCTGCAGGTGCAACTTCTC

Supplemental Table S3. Patient data for human heart samples
 DCM – dilated cardiomyopathy, ISCH – ischemic heart failure
 HF - heart failure cardiac fibroblast, HF - heart failure

<u>Sample #</u>	<u>Gender</u>	<u>Age</u>	<u>Health Status</u>
HFCF1	M	61	ISCH
HFCF2	M	62	ISCH
HFCF3	M	61	ISCH
Healthy heart tissue 1	M	58	
Healthy heart tissue 2	M	44	
Healthy heart tissue 3	F	43	
Healthy heart tissue 4	M	64	
Healthy heart tissue 5	M	40	
Healthy heart tissue 6	M	38	
Healthy heart tissue 7	F	46	
Healthy heart tissue 8	F	37	
Healthy heart tissue 9	M	60	
Healthy heart tissue 10	M	42	
Healthy heart tissue 11	F	61	
Healthy heart tissue 12	M	50	
Healthy heart tissue 13	F	44	
Healthy heart tissue 14	M	50	
Healthy heart tissue 15	F	60	
Healthy heart tissue 16	M	33	
Healthy heart tissue 17	F	67	
HF1	F	60	DCM
HF2	M	61	DCM
HF3	F	42	DCM
HF4	M	64	DCM
HF5	M	33	DCM
HF6	F	45	DCM
HF7	M	44	DCM
HF8	M	50	DCM
HF9	M	41	DCM
HF10	F	38	DCM
HF11	M	50	DCM
HF12	F	67	DCM
HF13	F	61	DCM
HF14	M	58	DCM
HF15	M	38	DCM

Figure 6a
NRF2 nuclear



1 2 3 4

1 2 3 4

1 2 3 4

L

Figure 6a
NRF2 cytoplasmic

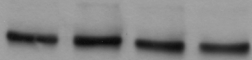


1 2 3 4

1 2 3 4

1 2 3 4

Lamin A/C



7

Figure 6a
nuclear
lamin A/C

Figure 6a
cytoplasmic
lamin A/C



β -tubulin
55kd

50kd

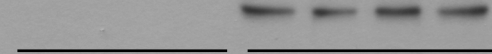


Figure 6a
nuclear
beta tubulin

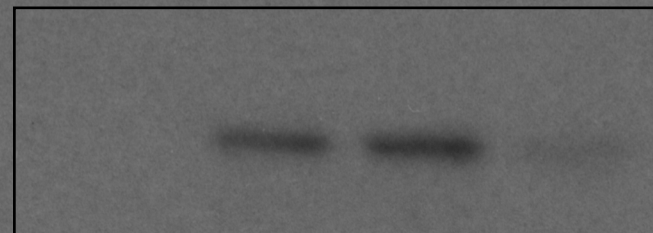
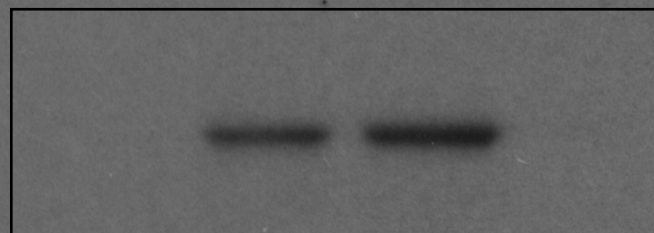
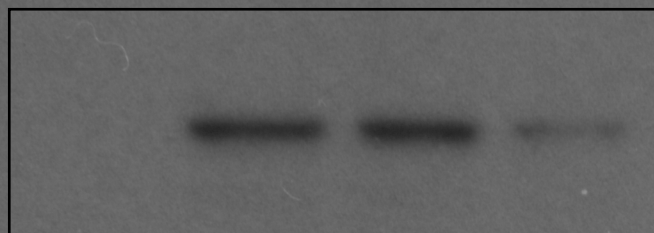
Figure 6a
cytoplasmic
beta tubulin

Nuclear NRF2 used for quantification in Fig. 6B

Experiment 1

Experiment 2

Experiment 3



C ROS I-ROS T-ROS

C ROS I-ROS T-ROS

C ROS I-ROS T-ROS

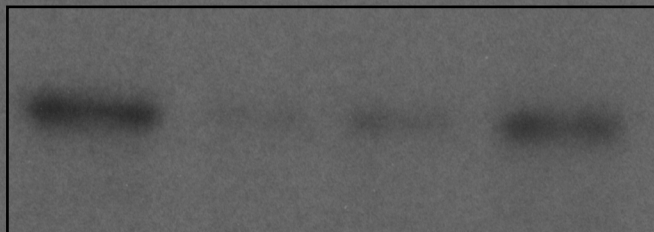
1 2 3 4

1 2 3 4

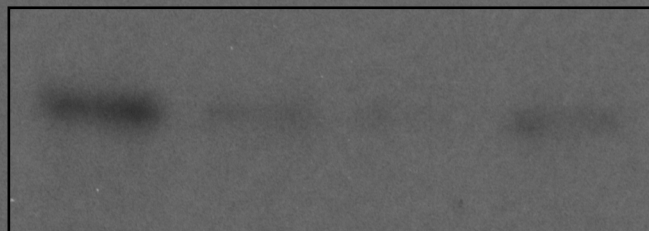
1 2 3 4

Cytoplasmic NRF2 used for quantification in Fig. 6B

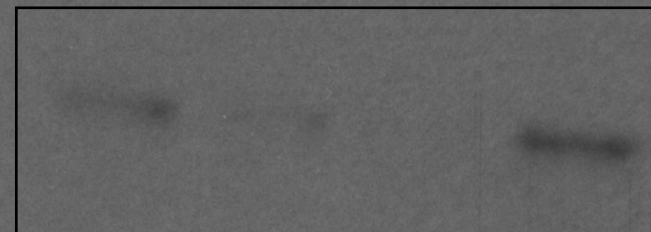
Experiment 1



Experiment 2



Experiment 3



C ROS I-ROS T-ROS

1 2 3 4

C ROS I-ROS T-ROS

1 2 3 4

C ROS I-ROS T-ROS

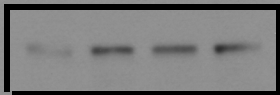
1 2 3 4

full unedited gel for
Supp Fig 4



Supp Fig 4a
pY-SMAD2/3

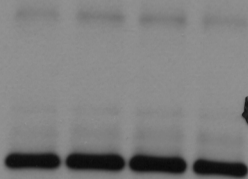
Full unedited gel for
Supp Fig 4



Supplemental Figure 4a
p473-AKT

Full unedited gel for
Supp Fig 4

7



tAKT

Supplemental Figure 4a
total AKT

Full unedited gel for
Supp Fig 4

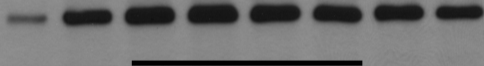


Supp Fig 4a
total SMAD



Supp Fig 4c
GAPDH

control
ROS
IGF/ROS
TGF/ROS



Full unedited gel for Supp Fig 4



TCL: NRF2



Supp Fig 4c
NRF2



IP: NRF2
IB: UB

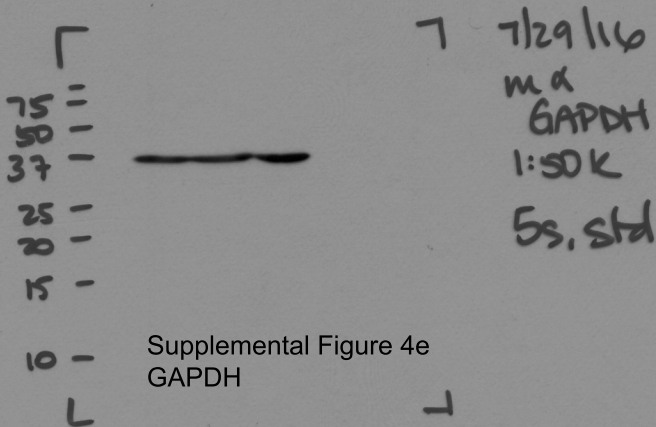
+ MG132

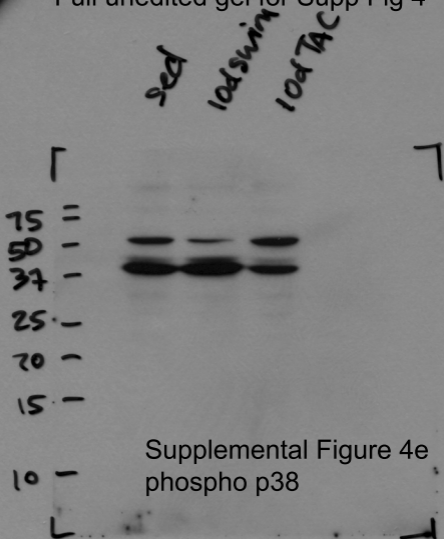


Supp Fig 4c
Ubiquitinated NRF2



Full unedited gel for Supp Fig 4



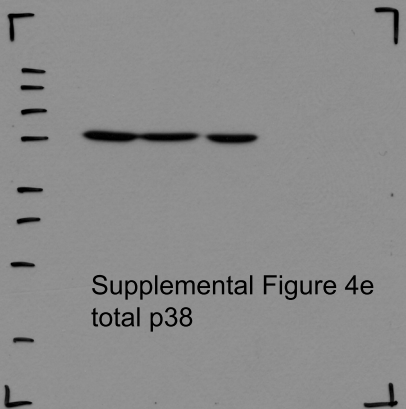


Supplemental Figure 4e
phospho p38

CF - 30mg

Full unedited gel for Supp Fig 4

7/28/14
309 std
Rbx total p38
9212 CST
1:1000



Supplemental Figure 4e
total p38